ESD-TR-71-318

ACCESSION LIST
Call No. 75011
Copy No. 1 of 1 cys.

ESD RECORD COPY
RETURN TO
SCIENTIFIC & TECHNICAL INFORMATION DIVISION
(TRI), Building 1210

ERI FILE COPY

Technical Note 1971-49

J. O. Dimmock

Capabilities and Limitations of Infrared Vidicons vs Infrared Scanning Systems

3 December 1971

Prepared under Electronic Systems Division Contract F19628-70-C-0230 by

Lincoln Laboratory
MASSACHUSETTS INSTITUTE OF TECHNOLOGY
Lexington, Massachusetts

AD0735324

Approved for public release; distribution unlimited.

MASSACHUSETTS INSTITUTE OF TECHNOLOGY

LINCOLN LABORATORY

CAPABILITIES AND LIMITATIONS OF INFRARED VIDICONS VS INFRARED SCANNING SYSTEMS

J. O. DIMMOCK

Group 85

TECHNICAL NOTE 1971-49

3 DECEMBER 1971

Approved for public release; distribution unlimited.

LEXINGTON MASSACHUSETTS

The work reported in this document was performed at Lincoln Laboratory, a center for research operated by Massachusetts Institute of Technology, with the support of the Department of the Air Force under Contract F19628-70-C-0230.

This report may be reproduced to satisfy needs of U.S. Government agencies.

ABSTRACT

The performances of infrared television camera tubes and infrared scanning systems are compared as a function of background photon flux density. The two-dimensional vidicon is found to be superior in performance at low background photon flux levels, below about 10^{12} photons/sec cm^2. At higher background levels, for application to terrestrial scenes in the 3 to 5 μm region (flux densities of $\sim 10^{13}$ to 10^{16} photons/sec cm^2) the two-dimensional vidicon is generally less sensitive than the linear array if variations in the vidicon target responsivity exceed about 0.05%. In addition, background suppression or compensation must be achieved through the use of either an electron flood beam or a photoconductive-photoemissive tube. Even if this is done, the contrast available in the vidicon appears marginal for terrestrial scenes. The situation in the 8 to 14 μm range (flux densities of 10^{18} photons/sec cm^2) is two orders of magnitude more difficult.

Accepted for the Air Force
Joseph R. Waterman, Lt. Col., USAF
Chief, Lincoln Laboratory Project Office

CAPABILITIES AND LIMITATIONS OF INFRARED VIDICONS VS. INFRARED SCANNING SYSTEMS

I. Introduction

This note compares the theoretical performance of infrared television camera tubes with infrared scanning systems as a function of background photon flux density. Specifically, we compare an infrared vidicon with m resolution lines and n resolution elements per line with a linear array of n elements being scanned across the scene. The vidicon target is read out by a scanning electron beam either directly into a video amplifier or is operated in the return beam mode in which the electron beam reflected off the target is amplified by an electron multiplier stage prior to the video amplifier. Each element in the linear array is connected directly to its own relatively narrow band amplifier. In addition, the performance of a linear vidicon is considered. This device consists of a linear array of n elements read out by a scanning electron beam as in the case of the two-dimensional vidicon. Both the linear array and linear array vidicon are mechanically scanned across the scene to provide a two-dimensional field of view.

The performance of infrared television-camera tubes and that of a single infrared detector scanned across the scene in a raster pattern to obtain an image has been previously analyzed by Hall.[1] The difference between this analysis and the one described below are: 1) Hall considered for comparison a single element infrared detector scanned in two directions where we consider a linear array scanned in one direction. 2) We compare the sensitivities of the systems at equal information rates, whereas Hall considered a lower information rate for the scanned single element, 100 kHz vs. 4.5 MHz for the vidicon. 3) We assume the ability to suppress or compensate for a uniform high flux density background through the use of a flood

beam or a photoconductive-photoemissive tube. Hall concluded that at flux densities below about 7×10^{12} photons/sec cm^2 the infrared vidicon is superior and that at flux densities above 1.26×10^{15} photons/sec cm^2 the scanned single element is better. In the intermediate flux density region there is a tradeoff between the two systems depending on the minimum detectable contrast of the scanner. These conclusions are very similar to those developed below, and in addition we conclude that the use of background suppression or compensation does not materially help, provided the vidicon target non-uniformities exceed 0.05%.

II. Analysis[2]

A. Background limit*

1. Two-dimensional vidicon

The background generation noise current for the two-dimensional vidicon can be calculated by considering a single element in the array. The number of photons which arrive at a single element in a frame time t is given by

$$N = \varphi_b t \tag{1}$$

where φ_b is background photon flux on the element. This is related to the background photon flux density Q_b by

$$\varphi_b = \frac{Q_b A_D}{4F^2} \tag{2}$$

where A_D is the single element area and F is the f-number of the optical system.

---

*This analysis assumes background generation current only, appropriate for a sensor consisting of an array of photodiodes. If the sensor consists of an array of photoconductors there is also recombination noise, and the noise current should be multiplied by $\sqrt{2}$.

The random fluctuation in N is

$$\sqrt{N} = \left(\frac{Q_b A_D}{4F^2} t \right)^{\frac{1}{2}} \quad . \tag{3}$$

The single element is read out by the scanning electron beam in a time τ approximately given by

$$\tau = t/M \tag{4}$$

where M is the total number of resolution elements, M = m rows x n elements per row. Assuming a unit quantum efficiency for conversion of photons into electrons the noise current is given by

$$i_N = q\sqrt{N}/\tau \tag{5}$$

where q is the charge on the electron. Combining Eqs. (3), (4), and (5)

$$i_N = \left(\tfrac{1}{2} q^2 \frac{Q_b A_D}{F^2} M^2 B \right)^{\frac{1}{2}} \tag{6}$$

where B is related to the system frame time t by

$$B = \frac{1}{2t} \tag{7}$$

We can replace the single element detector area in Eq. (6) by the total target area $A_T = MA_D$. This is further related to the system focal length f, the field-of-view Ω_{FOV} and the primary optics diameter D, by

$$\frac{A_T}{F^2} = \frac{A_T}{f^2} D^2 = \Omega_{FOV} D^2 \tag{8}$$

Consequently, we obtain for the background limited two-dimensional vidicon

$$i_N = (\tfrac{1}{2} q^2 Q_b \Omega_{FOV} D^2 MB)^{\frac{1}{2}} \tag{9}$$

The signal current can be calculated in a similar manner. Assume a signal flux φ_s on a single element. In analogy to Eq. (1) we obtain

$$S = \varphi_s t \tag{10}$$

which gives a signal current

$$i_s = qs/\tau \tag{11}$$

Using Eq. (4)

$$i_s = q\, M\varphi_s \quad . \tag{12}$$

The signal-to-noise ratio thus increases as $M^{\frac{1}{2}}$ as expected. This ratio also agrees with that calculated previously.[3]

2. Linear array (analysis for a single element)

For a single element in a linear array of n elements scanned across the scene perpendicular to the array a similar analysis gives

$$N = \varphi_b\, t/m \tag{13}$$

for m lines per frame. The read time is equal to t/m so that instead of Eq. (6) we have

$$i_N = \left(\tfrac{1}{2} q^2 \frac{Q_b A_D}{F^2}\, m\, B\right)^{\frac{1}{2}} \tag{14}$$

or replacing A_D by $A_T = MA_D = m \cdot nA_D$ and using Eq. (8) we obtain for a single element in the background limited linear array

$$i_N = (\tfrac{1}{2} q^2 Q_b\, \Omega_{FOV}\, D^2\, B/n)^{\frac{1}{2}} \tag{15}$$

The signal current is not integrated and is consequently given by

$$i_s = q\varphi_s \quad . \tag{16}$$

The signal-to-noise ratio increases as $n^{\frac{1}{2}}$ as expected. This ratio also agrees with that calculated previously.[3] The signal-to-noise ratio is reduced from that

of the two-dimensional vidicon by $m^{\frac{1}{2}}$. The multiplexed signal and noise currents are each multiplied by n, the number of elements in the array, giving

$$i_N\,(\text{Total}) = (\tfrac{1}{2}\, q^2\, Q_b\, \Omega_{FOV}\, D^2\, nB)^{\frac{1}{2}} \tag{15a}$$

$$i_s\,(\text{Total}) = qn\varphi_s \quad . \tag{16a}$$

3. Linear vidicon

The analysis proceeds in a similar manner for a single element in the array except the read time is equal to t/M. Instead of Eq. (14) we have

$$i_N = \left(\tfrac{1}{2}\, q^2\, \frac{Q_b A_D}{F^2}\, \frac{M^2}{m}\, B\right)^{\frac{1}{2}} \tag{17}$$

and Eq. (15) is replaced by

$$i_N(\tfrac{1}{2}\, q^2\, Q_b\, \Omega_{FOV}\, D^2\, n\, B)^{\frac{1}{2}} \tag{18}$$

which represents an increase in noise current over a single element in the linear array by n. However, the signal current is also increased by this factor because of the difference in write and read times M/m = n, so that

$$i_s = qn\varphi_s \tag{19}$$

and the signal-to-noise ratio also increases as $n^{\frac{1}{2}}$. Equations (18) and (19) are identical to those of the linear array after the signals from the n individual elements are multiplexed [Eqs. (15a) and (16a)]. In the case of the linear vidicon the scanning electron beam multiplexes the individual signals. The signal-to-noise ratio is the same as for the linear array.

B. Amplifier limit

1. Two-dimensional vidicon

The effective bandwidth for the amplifier in the vidicon system

is given by B times the number of resolution elements desired, $M = m \cdot n$. The noise current due to the amplifier can be expressed in a number of different forms, for example

$$i_N = \left(\frac{4k(T_a+T_L)}{R_L} MB \right)^{\frac{1}{2}} \tag{20}$$

where R_L is the load resistance, T_a is the equivalent input temperature of the amplifier and T_L is the temperature of the load resistor. Amplifier noise is frequently quoted in terms of a noise figure, NF, in units of dB referenced to the load resistor at 290°K. In terms of this, T_a is given by

$$T_a = 290\,(10^{NF/10} - 1)\,. \tag{21}$$

The value of the load resistor is limited by the total bandwidth required, MB, and the total input capacitance C_i, by

$$R_L \simeq \frac{1}{2\pi MBC_i} \quad . \tag{22}$$

With this Eq. (20) becomes

$$i_N = \left(8\pi k\,(T_a+T_L)\,C_i\,M^2B^2 \right)^{\frac{1}{2}} \tag{23}$$

The target-to-ground capacitance for a typical 2-inch return-beam vidicon[4] is approximately 18 pF which is increased by the transistor capacitances to $C_i \simeq$ 30 pF. Note that in the amplifier limit the signal-to-noise ratio is independent of M except that T_a is likely to be larger for very wide bandwidth systems.

2. Linear array (analysis for single element)

In analogy to Eq. (23) we have

$$i_N = \left(8\pi k\,(T_a+T_L)\,C_i\,m^2B^2 \right)^{\frac{1}{2}} \tag{24}$$

for a bandwidth of mB. At this lower bandwidth T_a may be somewhat less than in

the case of the vidicon and C_i will be less but probably not less than 10 pF determined by the transistor amplifier.

3. Linear Vidicon

The noise current in this case is given by Eq. (23) and is equal to that of the two-dimensional vidicon except that C_i may be less. We will assume C_i = 15 pF for system comparisons.

C. Return beam shot noise limit

At sufficiently low backgrounds the vidicon sensitivity can be improved by operating it in the return beam mode in which the electron beam which is reflected off the target is measured to determine the signal. This reflected beam is amplified in an electron multiplier section which can provide relatively noiseless gains up to about 1000 prior to the amplifier stage. In this case the signal is actually the reduction in beam current which occurs when the infrared radiation falls on the target. The noise current is given approximately by[5]

$$i_N = (2q\, I_b{}'\, MB/\tau_m\, K)^{\frac{1}{2}} \tag{25}$$

where $I_b{}'$ is the total read beam current, τ_m is a mesh transmission factor and K is another factor close to unity. $I_b{}'$ is proportional to the total target current I which we can assume is the discharge current due to the background. Typically, $I_b{}'$ will be 2 to 3 times the target current[6] and τ_m will be somewhat less than unity but probably greater than 0.5 so that Eq. (25) can be approximated by

$$i_N \simeq (12q\, I\, MB)^{\frac{1}{2}} \,. \tag{26}$$

The target current is related to the background flux density by

$$I = q\,\frac{Q_b A_T}{4F^2} \tag{27}$$

so that using Eq. (8), Eq. (26) becomes

$$i_N \simeq (3q^2 Q_b \Omega_{FOV} D^2 MB)^{\frac{1}{2}} \tag{28}$$

which is a factor of $\sqrt{6}$ greater than the background limited noise given by Eq. (9).

D. Detector noise limit

1. Two-dimensional vidicon

The detector noise limited current for a single element in the array is given by

$$i_N = q\left(\frac{\lambda}{hc}\right) \frac{(A_D B)^{\frac{1}{2}}}{D_\lambda^*} \tag{29}$$

where λ is the wavelength at which D_λ^* is measured. This noise is amplified by a factor of M in reading the target, so that using Eq. (8) the total detector noise limited current for the two-dimensional vidicon is

$$i_N = q\left(\frac{\lambda}{hc}\right) f\,(\Omega_{FOV} MB)^{\frac{1}{2}}/D_\lambda^* \tag{30}$$

where f is the optics focal length.

2. Linear array (analysis for single element)

$$i_N = q\left(\frac{\lambda}{hc}\right) \frac{(A_D mB)^{\frac{1}{2}}}{D_\lambda^*} \tag{31}$$

or

$$i_N = q\left(\frac{\lambda}{hc}\right) f\,(\Omega_{FOV} B/n)^{\frac{1}{2}}/D_\lambda^* \tag{32}$$

For the same D_λ^* the signal-to-noise ratio is reduced by a factor of $(M/n)^{\frac{1}{2}} = m^{\frac{1}{2}}$, the ratio of detector elements as in the background limited case.

3. Linear Vidicon

For a single element in the array i_N is given by Eq. (31). This is amplified by a factor of n giving

$$i_N = q\left(\frac{\lambda}{hc}\right) f\,(\Omega_{FOV}\, nB)^{\frac{1}{2}} / D^*_\lambda \tag{33}$$

so that the signal-to-noise ratio is the same as for the linear array.

III. Examples

In order to accomplish a real comparison between the vidicon infrared camera tube, the linear vidicon and the linear array, it is necessary to assume some specific system examples. The important system parameters are the frame time t, the field of view, Ω_{FOV}, the optics diameter D and the number of resolution elements M. There is a limiting relationship between these last three factors which is determined by the diffraction of the optics. The diffraction limited minimum resolution element size is given by

$$d \geq 2.4\, F\lambda \tag{34}$$

and

$$\frac{Md^2}{f^2} = \Omega_{FOV} \tag{35}$$

so that

$$\frac{\Omega_{FOV}\, D^2}{M} \geq (2.4\,\lambda)^2 \tag{36}$$

must be satisfied. The final additional consideration is the signal flux φ_s which is given by

$$\varphi_s = Q_s \frac{\pi}{4} D^2 \tag{37}$$

where Q_s is the incident signal flux density. In general, one would like to maximize φ_s, which dictates a large optics diameter subject to practical constraints, maximize Ω_{FOV} and maximize M.

A. Standard Video System

$m = n = 500$

$M = 250,000$

$t = 1/30$

$\Omega_{FOV} = 0.1 \times 0.1 \text{ rad} = 0.01 \text{ sr.}$

$D = 25 \text{ cm}$

$F = 1.5$

$A_T = 3.75 \times 3.75 \text{ cm} = 14 \text{ cm}^2$

$d = A_D^{\frac{1}{2}} = 75 \ \mu m$

$MB = 3.75 \text{ MHz}$

This combination satisfies Eq. (36) for $\lambda \leq 21 \ \mu m$. Substituting these values into Eqs. (9), (15) and(18) yields for the background limits:

Vidicon

$$i_N = 5.5 \times 10^{-16} \, Q_b^{\frac{1}{2}} \text{ (amps)}$$

linear array

$$i_N = 4.9 \times 10^{-20} \, Q_b^{\frac{1}{2}} \text{ (amps)}$$

linear vidicon

$$i_N = 2.45 \times 10^{-17} \, Q_b^{\frac{1}{2}} \text{ (amps)}$$

Q_b in $cm^{-2} \, sec^{-1}$.

The vidicon amplifier bandwidth is MB = 3.75 MHz. Noise currents for low noise preamplifiers with this bandwidth range from 1 to 2 nA.[1,4] Equation (22) gives a

value of $R_L = 1.4\ k\Omega$. Using Eq. (20) we calculate a noise equivalent amplifier temperature of 6.84^oK for $i_N = 1$ nA and 27.4^oK for $i_N = 2$ nA. Assuming the higher noise figure and including the temperature of the load resistor we obtain

$$i_N(\text{amp}) = 2.5 \times 10^{-9}\ A$$

for the vidicon with $T_L = 15^oK$ and

$$i_N\ (\text{amp}) = 4 \times 10^{-9}\ A$$

for the vidicon with $T_L = 80^oK$.

The amplifier bandwidth for a single element in the linear array is mB = 7.5 kHz. Amplifiers with noise figures as low as 0.02 dB,[7] $T_a = 1.3^oK$ are available in this frequency range so that the amplifier noise can be neglected compared to the load resistor noise. Using Eq. (24) with $C_i = 10$ pF we obtain for the linear array

$$i_N\ (\text{amp}) = 1.7 \times 10^{-12}\ A$$

for $T_L = 15^oK$ and

$$i_N(\text{amp}) = 3.95 \times 10^{-12}\ A$$

for $T_L = 80^oK$.

For the linear vidicon, assuming $C_i = 15$ pF we obtain

$$i_N(\text{amp}) = 1.77 \times 10^{-9}\ A$$

for $T_L = 15^oK$, and

$$i_N(\text{amp}) = 2.82 \times 10^{-9}\ A$$

for $T_L = 80^oK$.

The return beam vidicon shot noise current is

$$i_N(\text{shot}) = 1.35 \times 10^{-15}\, Q_b^{\frac{1}{2}} \text{ (amps)}$$

and for the linear vidicon

$$i_N(\text{shot}) = 6.02 \times 10^{-17}\, Q_b^{\frac{1}{2}} \text{ (amps)}$$

again Q_b in $cm^{-2}\ sec^{-1}$.

The detector limited noise current for the vidicon is

$$i_N(D_\lambda^*) = 5.86 \times 10^3\, \lambda/D_\lambda^* \text{ (amps)}$$

where λ is in μm and D_λ^* is in $cmHz^{\frac{1}{2}}/Watt$. For the linear array

$$i_N(D_\lambda^*) = 0.524\lambda/D_\lambda^* \text{ (amps)}$$

and for the linear vidicon

$$i_N(D_\lambda^*) = 2.62 \times 10^2\, \lambda/D_\lambda^* \text{ (amps)}$$

A plot of these results is shown in Fig. 1. The noise current for the linear array is scaled up by a factor of M = 250,000 and that of the linear vidicon is scaled up by a factor of m = 500 to account for the difference in signal current for comparison with the two-dimensional vidicon. The detectivity requirements for the linear array and linear vidicon for λ = 14, 5, and 2.5 μm are indicated on the left of the figure. These values give the lower limit for the equivalent noise current determined by the detector noise. For example, a linear vidicon of 5 μm detectors with detectivities of 10^{13} $cmHz^{\frac{1}{2}}/W$ would be return beam shot noise limited down to background photon flux densities of about 4.5×10^{12} photons/sec cm^2 where the shot noise equals the detector noise of 6.6×10^{-8} A. The detector noise limit for the two-dimensional vidicon is $\sqrt{m}$ times lower, or $i_N = 2.93 \times 10^{-9}$ A which is in the crossover region between the vidicon amplifier limit and the return beam vidicon shot noise limit. In both the shot

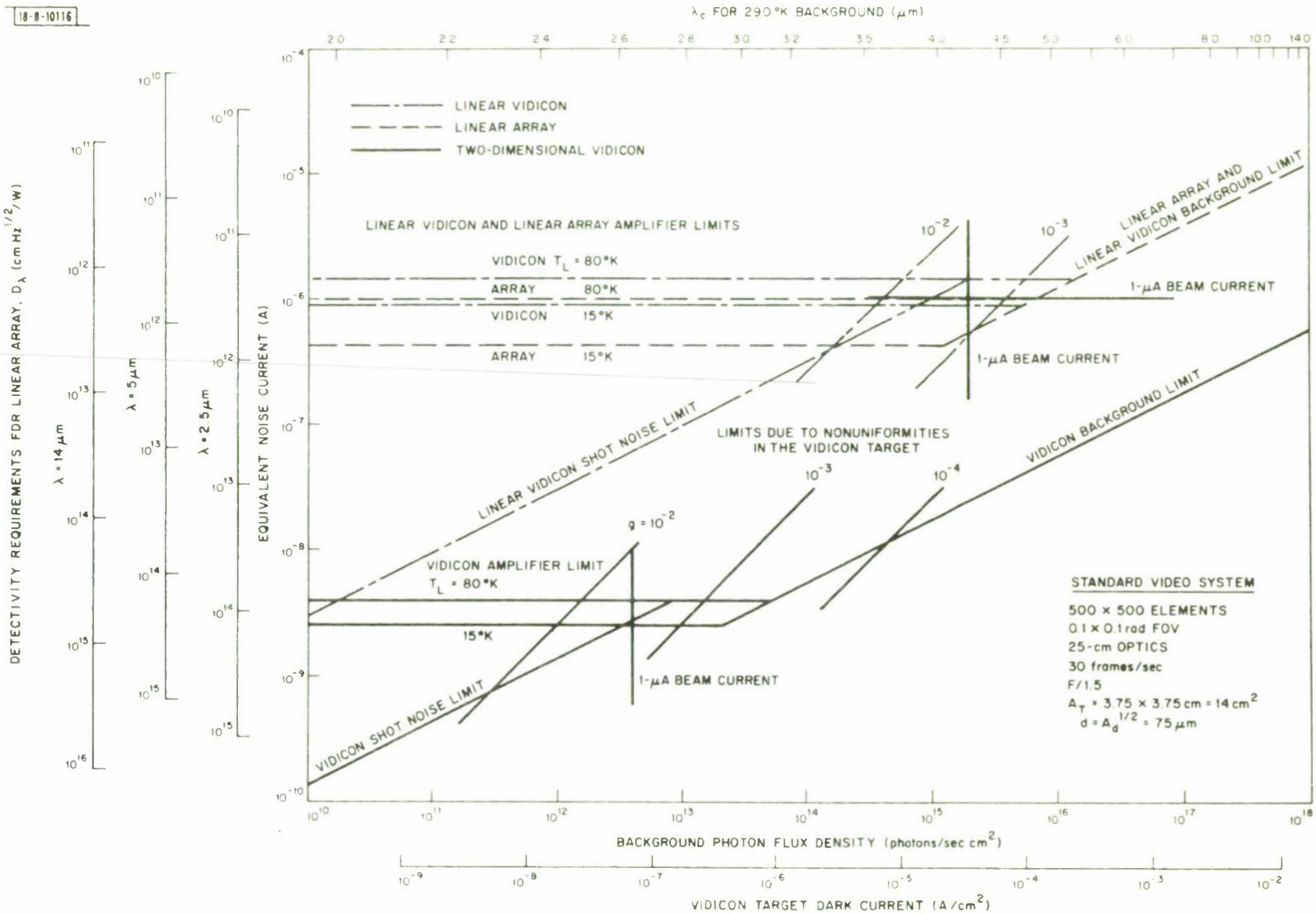

Fig. 1. Standard video system.

noise and background limited regimes the curves for the linear and two-dimensional vidicons are scaled by $\sqrt{m}$ such that for a given target element detectivity both systems become detector limited at the same background photon flux density.

In addition, in the case of an ideal diode array, the detector noise current is given by the shot noise due to the diode reverse bias leakage or dark current. The detector shot noise for a given dark current is equal to the background limited noise at that background photon flux density required to generate the detector dark current. Consequently, if the diode array does not display excess noise above this shot noise current, and the dark current is less than or equal to that generated by the background photon flux density, then the detector noise will be less than or equal to the calculated background limit. Since this background limit is equal to or less than the actual system noise current appropriate to a given background, the detector noise will be less than or equal to the total calculated noise for any of the systems. Therefore, if the diode array dark current is less than that corresponding to a given photon flux density, and the diodes do not display excess noise the system will not be detector noise limited but will be limited instead by one of the other noise mechanisms shown in the figure. The target dark current densities corresponding to the background photon flux densities are indicated on the lower horizontal axis $[i_d = qQ_b/4F^2 = 1.78 \times 10^{-20} Q_b \text{ (amps/cm}^2)]$. For a shot noise limited diode array, the low background performance can be determined directly from the array leakage or dark current per cm^2 using this scale and reading the noise currents as shown.

Also shown on the figure are the approximate noise current limits due to non-uniformities in the vidicon targets. If these non-uniformities are assumed to generate completely random noise then the value of the noise current is given by

$$i_N \text{ (target)} = g(qQ_b A_T/4F^2) \text{ (amps)} \tag{38}$$

$$= g(\tfrac{1}{4} q Q_b \Omega_{FOV} D^2) \text{ (amps)} \tag{39}$$

where g represents the rms variation in target uniformity (quantum efficiency, photoconductive gain, dark current, etc.). This limit applies to both the two-dimensional and linear vidicon unless some scheme is devised to cancel it out such as frame-to-frame difference comparisons or some form of spatial filtering. The problem can be largely avoided in the case of the linear array simply by first capacitively coupling the detector elements to the amplifiers, thus eliminating the dc dark or leakage current and second adjusting the individual amplifier gain to balance out differences in detector responsivities. Finally, we have indicated the background photon flux density at which the scanning electron beam current is equal to 1 μA. Hall[1] has indicated that this is an approximate practical limit such that operation at higher flux densities can only be accomplished through the use of background suppression, as in a photoconductive-photoemissive tube, compensation through the use of a flood beam or through the use of multiple scanning beams. These three approaches are discussed in Appendix A.

B. Low Bandwidth Narrow FOV System

$m = n = 100$

$M = 10,000$

$t = 1/10$

$\Omega_{FOV} = 0.02 \times 0.02 \text{ rad} = 4 \times 10^{-4} \text{ sr}$

$D = 25 \text{ cm}$

$F = 1.5, \; A_T = 0.75 \times 0.75 \text{ cm} = 0.56 \text{ cm}^2$

$d = A_D^{\frac{1}{2}} = 75 \; \mu\text{m}$

$MB = 50 \text{ kHz}$

The results for this system are shown in Fig. 2.

The two-dimensional vidicon background limit for this system is $i_N = 1.26 \times 10^{-17}$ $Q_b^{\frac{1}{2}}$ (amps), and that of the linear array and linear vidicon are effectively $\sqrt{m}$ = 10 times higher. For a 50 kHz vidicon bandwidth we estimate $T_a = 3^oK$ and assume a noise temperature of 1.5^oK for the 500 Hz bandwidth of a single element in the linear array. The two-dimensional vidicon shot noise limit is $\sqrt{6}$ times the background limit or 3.09×10^{-17} $Q_b^{\frac{1}{2}}$ (amp) and again the effective shot noise for the linear vidicon is 10 times greater than this. The detector noise limit for the linear array is $0.135\ \lambda/D_\lambda^*$ but is scaled up by a factor of $M = 10^4$ in Fig. 2 for proper comparison. The general results are similar to those for the standard video system displayed in Fig. 1 except that the limit of 1 μA electron beam current permits operation at somewhat higher background flux densities in the background limited regime because of the smaller target area.

C. Wide Bandwidth System

$m = n = 2000$

$M = 4 \times 10^6$

$t = 1/10$

$\Omega_{FOV} = 0.07 \times 0.07$ rad $= 4.9 \times 10^{-3}$ sr

$D = 100$ cm

$F = 1.5$, $A_T = 10.5 \times 10.5$ cm $= 110$ cm^2

$d = A_D = 52.5$ μm

MB = 20 MHz

The results for this system are shown in Fig. 3.

The two-dimensional vidicon background limit for this system is $i_N = 5.01 \times 10^{-15}$ $Q_b^{\frac{1}{2}}$ (amps), and that of the linear array and linear vidicon are effectively $\sqrt{m} = 44.7$ times higher. For a 20 MHz vidicon bandwidth we estimate $T_a = 65^oK$ and assume a noise temperature of 1.5^oK for the 10 kHz bandwidth for a single element in the

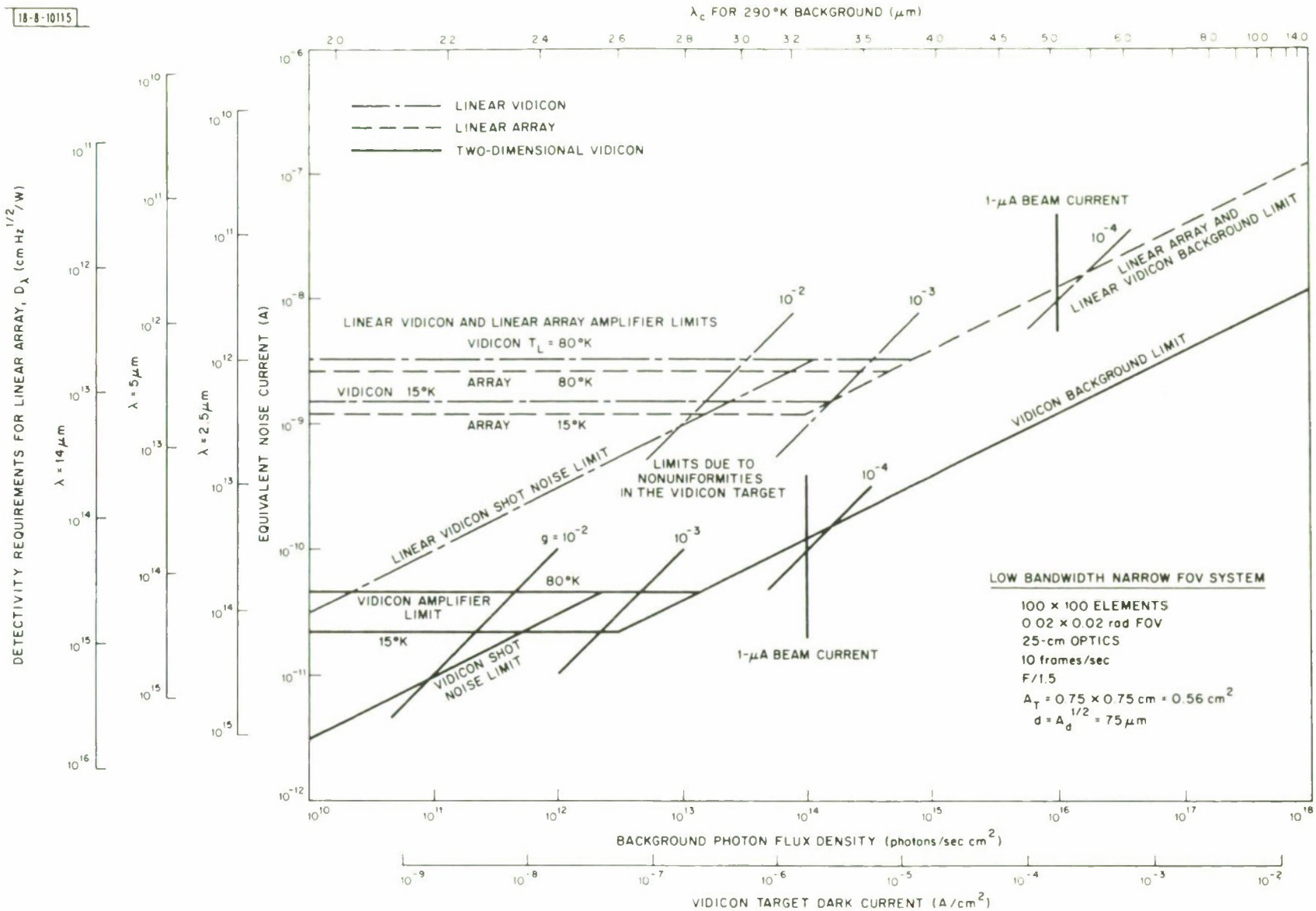

Fig. 2. Low bandwidth narrow FOV system.

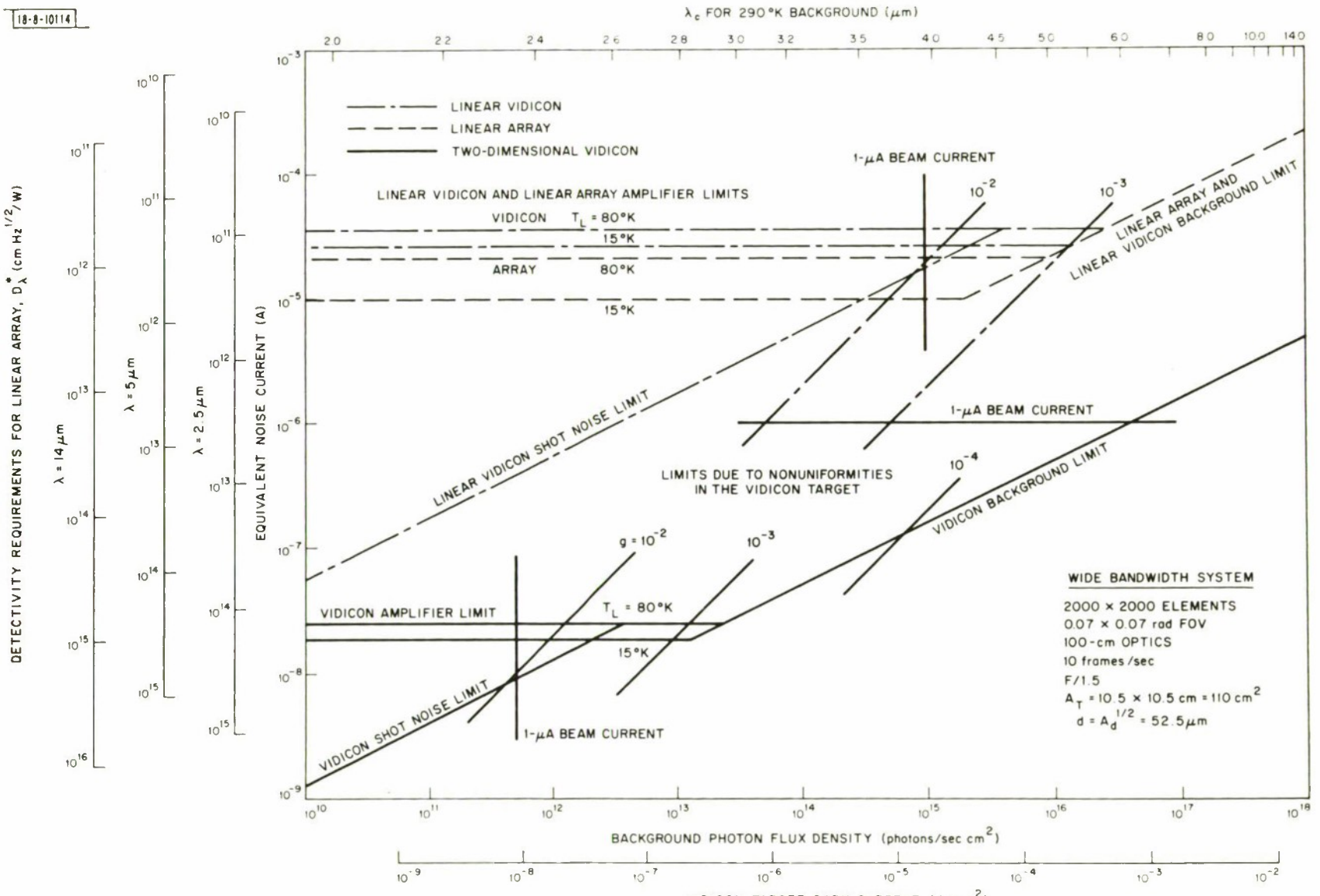

Fig. 3. Wide bandwidth system.

linear array. The two-dimensional vidicon shot noise limit is $\sqrt{6}$ times the background limit or $1.23 \times 10^{-14}\ Q_b^{\frac{1}{2}}$ (amp) and the effective shot noise for the linear vidicon is 44.7 times greater than this. The detector noise limit for the linear array is $0.423\ \lambda/D^*_\lambda$ but is scaled up by a factor of $M = 4 \times 10^6$ in Fig. 3 for proper comparison. The general results are similar to those displayed in Figs. 1 and 2 except that the limit of 1 μA electron beam current restricts operation to somewhat lower background flux densities because of the larger target area.

IV. Discussion, Conclusions and Recommendations

From the results given in Figs. 1, 2 and 3 several general conclusions can be drawn.

1. The linear vidicon and linear array in normal operation have comparable performances except for differences in target-to-ground capacitances and amplifier noise temperatures, and except for limitations in the linear vidicon due to target non-uniformities.

2. Operation of the linear vidicon in the return beam mode at low backgrounds allows it to become significantly more sensitive than the linear array.

3. The two-dimensional vidicon has potentially superior performance at all background levels provided that problems introduced by target non-uniformities can be reduced or eliminated and the 1 μA electron beam current limitation can be circumvented by background suppression or cancellation.

4. If target non-uniformities are less than 1% the two-dimensional vidicon is a very attractive device at backgrounds below about 10^{12} photons/sec cm^2. Operation in this region also presupposes a total vidicon target dark current less than approximately 10^{-8} A/cm^2.

With these qualitative conclusions it becomes important to explore how the potentially superior performance of the two-dimensional vidicon can be realized in the higher

background region above 10^{12} photons/sec cm^2. Figure 4 gives the total background photon flux density integrated over wavelengths from $\lambda = 0$ to $\lambda = \lambda_c$ a maximum cutoff wavelength vs λ_c for various background temperatures. It is clear from this that a ground-based system, $T_b \simeq 290^oK$, limited to $Q_b \leq 10^{12}$ photons/sec cm^2 is limited to $\lambda_c < 2.5$ μm. The corresponding cutoff wavelengths, λ_c, for $T_b = 290^oK$ are indicated on the top of Figs. 1-3. An atmospheric transmission spectrum is shown in Fig. 5. This indicates that a system limited to $\lambda_c \leq 2.5$ μm could cover only the near infrared region of this spectrum. However, the peak spectral radiant emittance for objects near ambient temperature occurs at longer wavelengths. Figure 6 shows the increase in spectral radiant emittance (signal) above that of a 300^oK background for various target temperatures. For target temperatures close to 300^oK, this differential radiant emittance has a peak at $\lambda = 8$ μm. Figure 7 shows the blackbody spectral radiant emittances for several blackbody temperatures. For $T_b = 290^oK$, $\lambda_{peak} \simeq 10$ μm which also indicates that longer wavelength response is desirable.

Let us consider what is necessary to extend the operative region of the two-dimensional vidicon to cover the 3 to 5 μm middle infrared atmospheric window for a background $T_b = 290^oK$. From Fig. 4 this corresponds to a background photon flux density of approximately 10^{16} photons/sec cm^2. Two factors hinder the accomplishment of this.

1. The 1 μA scanning electron beam current limit. This problem can be circumvented in principle by

   a. Continuously flooding the vidicon target with a uniform electron beam.

   b. Using a photoconductive-photoemissive tube with a retarding grid to suppress the background, or

   c. Using a multiple electron beam scan.

These three modifications to the standard vidicon are discussed in Appendix A.

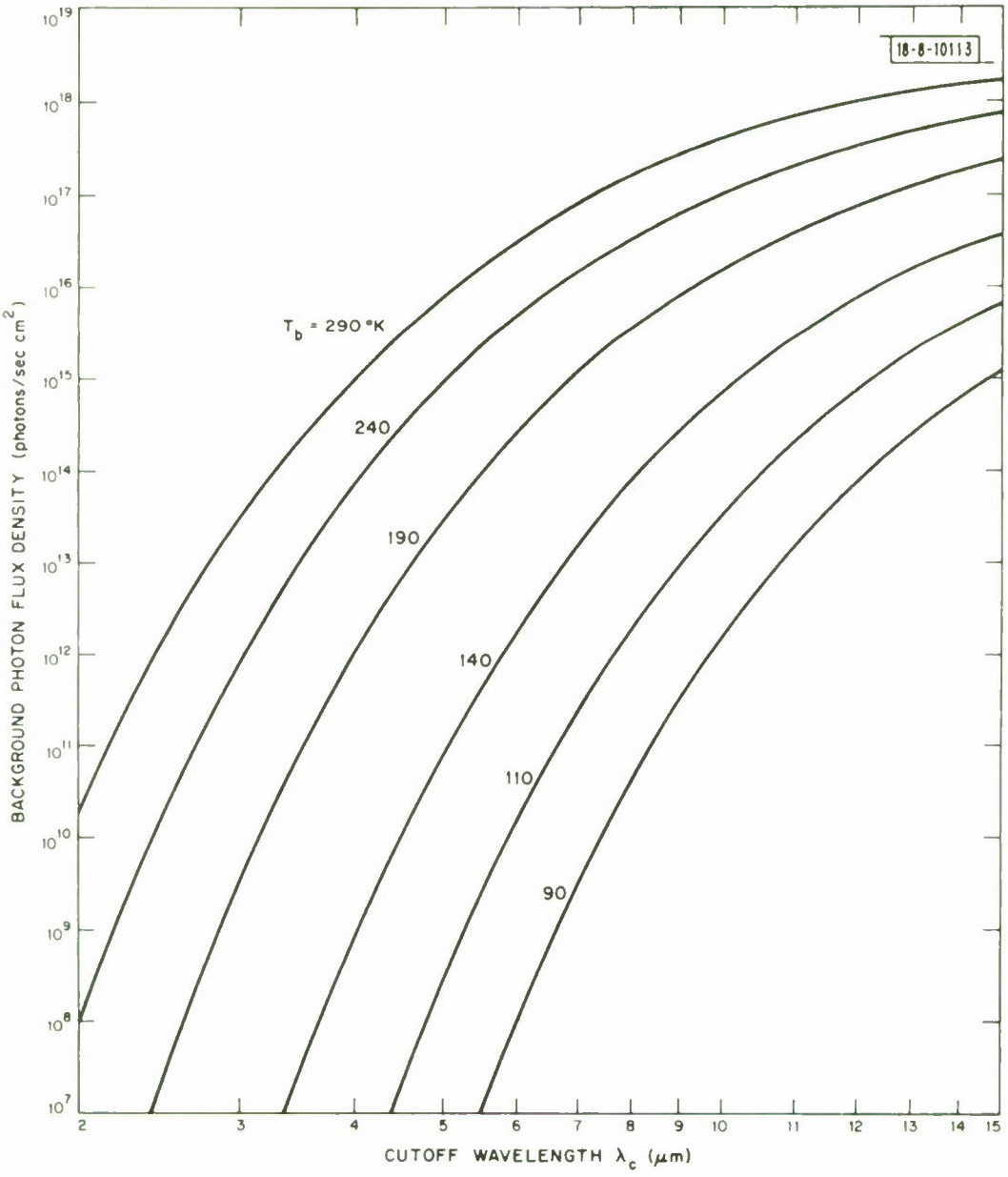

Fig. 4. Total background photon flux density for $\lambda \leq \lambda_c$ for various background temperatures.

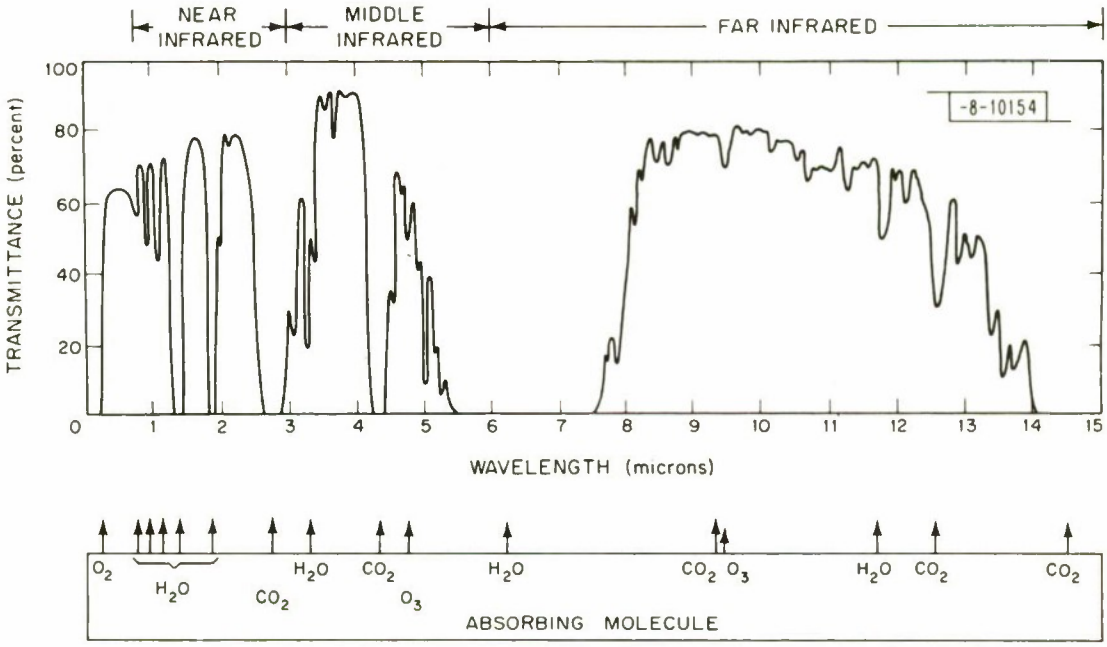

Fig. 5. Transmittance of the atmosphere for a 6000-foot horizontal path at sea level containing 17 mm of precipitable water.
(After R. D. Hudson, Jr., Ref. 8, p. 115.)

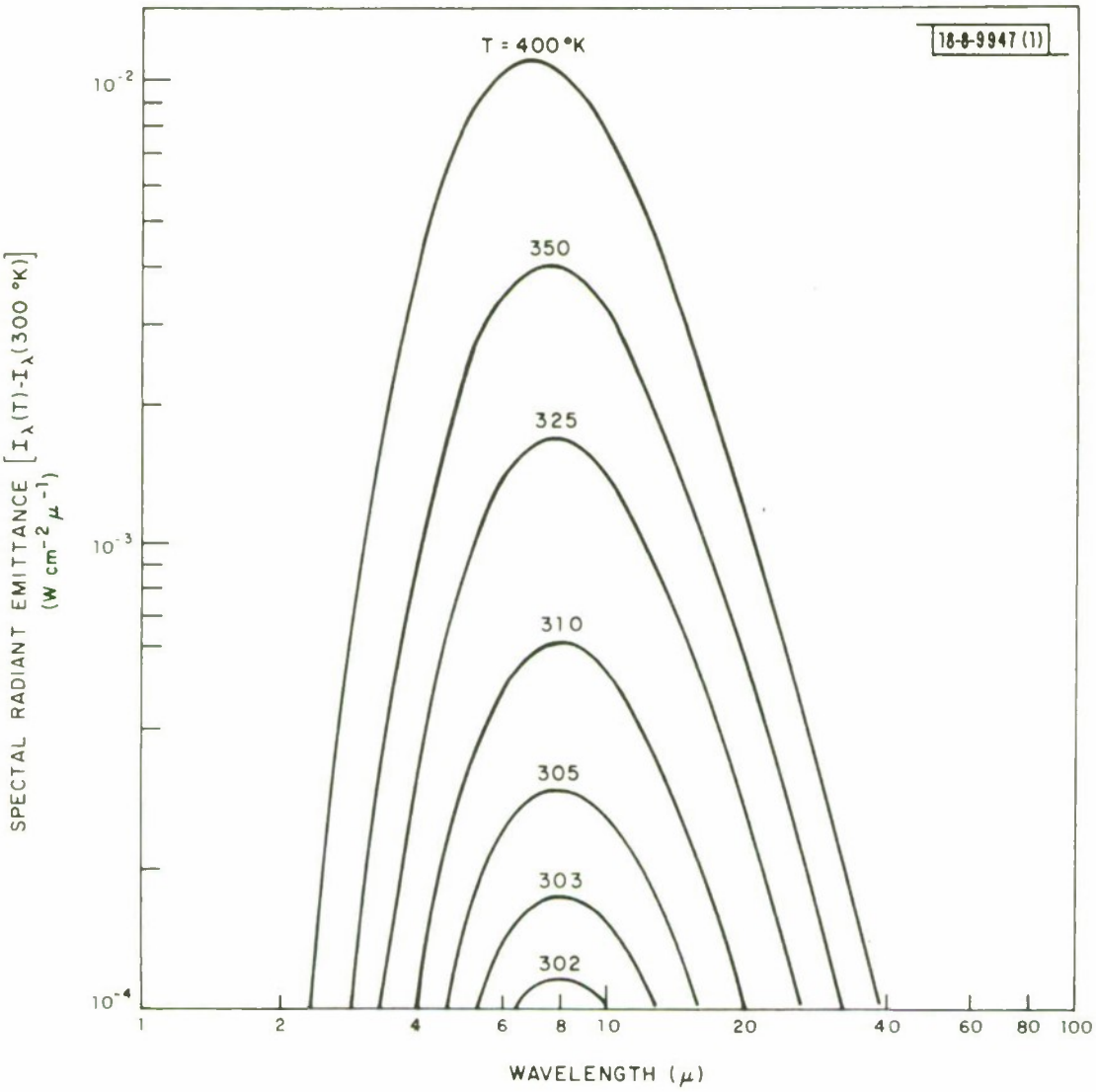

Fig. 6. Difference in spectral radiant emittance between that of a blackbody at the various indicated temperatures and that of a blackbody at 300°K as a function of wavelength.

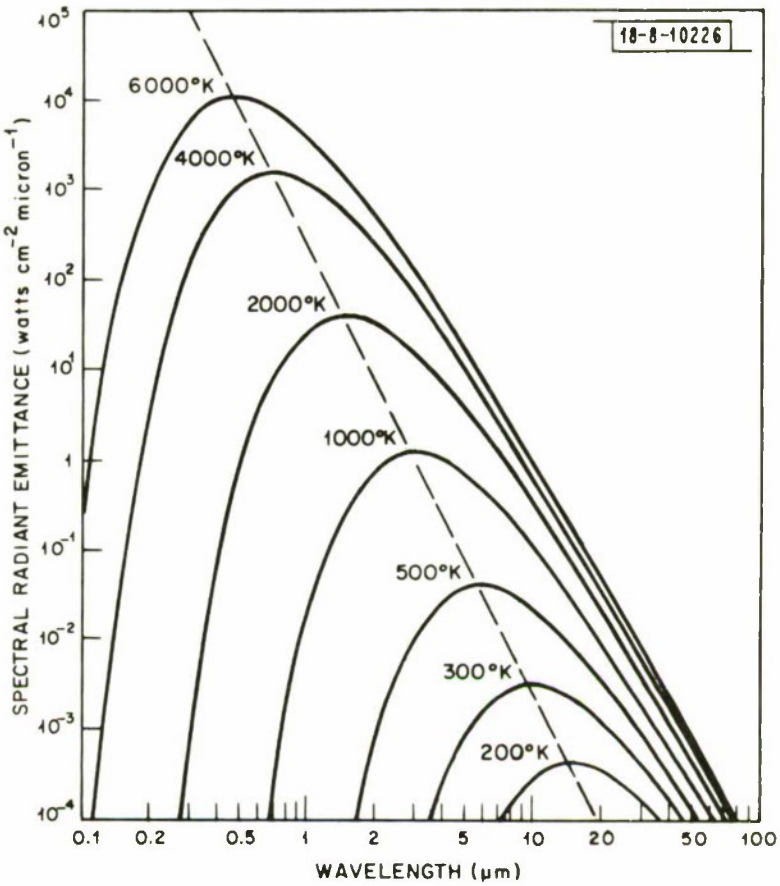

Fig. 7. Spectral radiant emittance of a blackbody at various temperatures as a function of wavelength. The maximum spectral radiant emittance at a given wavelength falls on the dashed curve.
(After J. A. Jamieson et al., Ref. 9, p. 20.)

Correlated with this problem is also the general inability of vidicon targets to store large amounts of charge. This limit varies with the type of target. This problem is circumvented by the flood beam and the photoconductive-photoemissive system but not by the multiple scanning beams.

b. The limitations due to non-uniformities in the vidicon target. The percentage variation in background flux with background temperature is approximately proportional to $1/\lambda_c$, where λ_c is the long wavelength cutoff (see Appendix B) and at $\lambda_c = 5\ \mu m$ is 3.8% per ^oK for $T_b = 290^oK$. The only obvious way of compensating for this is through the use of frame-to-frame comparisons. In the case of the flood beam this could be used to spatially modulate the flood in an attempt to compensate the non-uniformities. The effectiveness of this is bound to be severely limited in practice. There is no obvious way of utilizing this type of feedback in the case of either the photoconductive-photoemissive system or the multiple scanning electron beam system. Target and background non-uniformities consequently limit the amount of background suppression that can be achieved in these systems.

In order to ascertain to what degree a two-dimensional vidicon can be enabled to operate at higher background photon flux densities through the use of background suppression or compensation in a photoconductive-photoemissive or electron flood beam tube, let us consider specifically the standard video system depicted in Fig. 1. Without the use of background suppression or compensation the system is limited to background photon flux densities below 4×10^{12} photons/sec cm^2. The dominant noise is either amplifier or shot noise provided the target uniformity is better than 4×10^{-3}.

It is almost certain that the system will be subject to non-uniformities greater than this so these non-uniformities probably will be the limiting factor. If the

limiting noise factor at the operating photon flux level is due to inhomogeneities in the target responsivity then this noise is likely to increase linearly with the background photon flux density, as the system long wavelength cutoff is shifted to longer wavelengths. However, from Fig. B-1 it is seen that the relative signal due to a given temperature differential is less at longer wavelengths. Thus, the relative signal-to-noise ratio is reduced by the shift to longer wavelengths. This means that the optimum operating point is that background photon flux density at which the noise due to target non-uniformities is equal to the noise due to other sources. For the standard video system with a target inhomogeneity of 10^{-2} this point is 1.6×10^{12} photons/sec cm^2 for an 80°K amplifier limit or 2.8×10^{11} photons/sec cm^2 for the return beam shot noise limit. Since these operating points are both below the limit of 4×10^{12} photons/sec cm^2 set by the scanning electron beam current of 1 μA, the flood beam or background suppression is not helpful. For the vidicon 80°K amplifier limited noise of 4×10^{-8} A the system dynamic range is 250 ($1 \times 10^{-6}/4 \times 10^{-8}$), the optimum cutoff wavelength is 2.5 μm and the noise equivalent temperature differential is $\Delta T = 0.14^o$K. For the vidicon shot noise limit of 7×10^{-10} A the system dynamic range is 100 ($7 \times 10^{-8}/7 \times 10^{-10}$) due to the reduction in vidicon beam current, the cutoff wavelength is 2.3 μm and the noise equivalent temperature differential is $\Delta T = 0.13^o$K. If the noise due to target non-uniformities is less, then the system performance can be improved by flooding or suppressing the background and extending the long wavelength cutoff. For example, if the non-uniformities are 10^{-3} the optimum flux density is 1.6×10^{13} photons/sec cm^2 for an 80°K vidicon amplifier noise limit. The cutoff wavelength becomes 2.8 μm, the dynamic range is still 250 but the noise equivalent temperature differential is $\Delta T = 0.015^o$K. The system saturates at $\Delta T = 4^o$K. *

---

* Note, however, that the atmosphere is quite opaque between 2.5 and 2.8 μm (see Fig. 5), so that this is not realistic.

The two-dimensional vidicon operating in this near infrared region is a very sensitive system. It appears extremely difficult and of dubious value to attempt to significantly extend the wavelength of operation much beyond this range, at least for terrestrial application. The two-dimensional vidicon is thus limited to operation in the near infrared wavelength region (wavelengths less than $\lambda \simeq 2.5\ \mu m$) -- see Fig. 5. This limitation is effectively the same for all three systems considered here. Extremely high uniformity targets are required before operation at significantly longer wavelengths would be possible or result in increased sensitivity.

Let us compare the performance of the two-dimensional vidicon at 2.5 μm with that of a linear array with a long wavelength cutoff at 5 μm covering the middle 3-5 μm infrared region. At a background photon flux of 10^{16} photons/sec cm^2 the linear array is background limited at an equivalent noise current of $i_N = 1.2 \times 10^{-6}$ A. The noise equivalent temperature differential is $0.0125^{o}K$, and the dynamic range is essentially unlimited but at least as large as 2000 (the equivalent inhomogeneity is 4.8×10^{-4}). Thus, the linear array is both more sensitive and has a larger dynamic range. The detector sensitivity requirements are $D^*_\lambda \geq 1.6 \times 10^{11}\ cmHz^{\frac{1}{2}}/W$ for the 2.5 μm two-dimensional vidicon and $D^*_\lambda \geq 5.5 \times 10^{11}\ cmHz^{\frac{1}{2}}/W$ for the 5 μm linear array. The only advantage the two-dimensional vidicon has is the possibility of higher temperature operation, although this would increase the noise equivalent temperature differential and reduce the dynamic range.

The linear vidicon requires a uniformity of 4.8×10^{-4} to have a sensitivity (using a flood beam) equal to that of the linear array at 5 μm. For a linear vidicon uniformity of 10^{-2} the optimum flux density for operation is 6×10^{14} photons/sec cm^2, corresponding to a cutoff wavelength of $\lambda_c = 3.8\ \mu m$. The noise equivalent temperature differential is $\Delta T = 0.2^{o}K$ and the dynamic range is 360. Its sensitivity is nearly as good as and the dynamic range is somewhat larger than the two-dimensional vidicon.

All of the above discussion is based on the assumption that non-uniformities in the vidicon target responsivity introduce an uncorrelated noise current equal to the background flux generated current times the non-uniformity factor g. In fact, this is not an uncorrelated noise and therefore it can be compensated for at least in principle. This can be accomplished by a frame-to-frame comparison which would then show up changes in the incident flux. The system then becomes in effect a moving target indicator. Images of a stationary scene could be acquired by having the sensor view a uniform scene on alternate frames to provide a standard for frame-to-frame comparison. Alternatively, this could be improvised by proving a simulated image characteristic of the vidicon target non-uniformities for the comparison. All of this requires considerable real time data analysis and high speed $\sim$ 5 MHz computation and several megabits of high speed memory.

To the degree that this data processing can be used to reduce the noise introduced by vidicon target non-uniformities the system sensitivity will be improved and higher background operation will be possible and profitable. For example, if a vidicon target non-uniformity of 10^{-2} can be compensated to 1% by frame-to-frame comparison the noise would be equivalent to that of a system with a non-uniformity of 10^{-4}.

The optimum operating point for such a system would be at a background photon flux of 4.6×10^{14} photons/sec cm^2 or $\lambda_c = 3.6$ μm for the standard video system. The noise equivalent temperature differential is $\Delta T = 2 \times 10^{-3}$ ^{o}K and the dynamic range is 86 ($\Delta T = 0.17^{o}$K). This system is far too sensitive for most applications. Consider that we wish to view a scene with a maximum ΔT of 5°K corresponding to a differential in the background photon flux density of 4×10^{12} photons/sec cm^2 (1 μA beam current). For a 290°K background this corresponds to $\lambda_c = 2.8$ μm. Because of the atmospheric absorption band between 2.5 and 2.8 μm the range

should be extended to nearly 3 μm. For a dynamic range of 250 this gives a minimum temperature differential of 0.02^{o} K, slightly inferior to that of the linear array at 5 μm. Realization of this system requires an effective vidicon target uniformity including any data analysis compensation of 8×10^{-4} and flood beam background suppression of about 90%.

Summary

The two-dimensional infrared vidicon is potentially more sensitive than either the linear vidicon or the linear array, and it is definitively the superior system for low background applications: $\lambda_c \geq 2.6$ μm or space applications. The two-dimensional infrared vidicon is limited at higher backgrounds by the available electron beam current of ~ 1 μA, the dynamic range, maximum of 250 for the standard video system, and by target non-uniformities. These statements are approximately relevant for the standard video system. The uniformity requirements are about the same for the other two systems considered. The low bandwidth system does not require background suppression and has sufficient dynamic range, $\sim 10^4$. The wide bandwidth system requires considerably more background suppression, ~ 98 %, and has considerably less dynamic range, ~ 40. The electron beam current limitation can be partly circumvented by using an electron flood beam or a photo-conductive-photoemissive type of tube. The target non-uniformities can be partially compensated for by data analysis or frame-to-frame comparisons. For moderate contrast scenes, $\Delta T_{max} = 5^{o}$K, the dynamic range limits minimum differential temperature sensitivity to $\Delta T_{min} = 0.02^{o}$K, approximately equal to that of the linear array. The dynamic range and thus the minimum sensitivity can be increased by forming a number of images at different sensitivity using variable neutral density filters, for example. This is not necessary, of course, if the scene contrast is very low, $\Delta T_{max} \leq 0.2^{o}$K.

Thus, the two-dimensional infrared vidicon can have a sensitivity equal to or greater than that of a linear array for terrestrial scenes in the 3 to 5 μ m region if the effective target non-uniformity is low, $< 5 \times 10^{-4}$, background suppression is employed, and the dynamic range is adequate to handle the maximum scene contrasts. Competition in the 8 - 14 μm region is a two-order-of-magnitude more difficult problem and appears out of the question at present. Even the situation in the 3 to 5 μm region appears sufficiently difficult to warrant the question if the effort necessary to develop an infrared vidicon with sensitivity comparable to that of the linear array is worth it.

APPENDIX A

A. Flood Beam Vidicon

A schematic diagram of a flood beam vidicon is shown in Fig. A-1. In the simplest configuration, the flood beam density is essentially uniform across the target and the landing velocity would be adjusted such that the landing probability is nearly independent of the target surface potential. Under these circumstances, the flood beam acts as a constant current source. Considering a maximum current density available from an oxide-type thermionic cathode of about 1 A/cm^2 for a reasonable operating life,[1] a 1 x 1 mm cathode could deliver about 10 mA, four orders of magnitude more than the scanning electron beam.

From the above, it appears that the flood gun should enable the system to handle the high current generated by the infrared flux. This still leaves unanswered the question if the target could integrate the signal for a full frame time under these circumstances. It turns out that the answer is different for a photoconductor vs a photodiode target. The ideal current-voltage characteristic for a photoconductive target is shown schematically in Fig. A-2a and that of a photodiode in Fig. A-2b. The fundamental difference between these is that the high light level changes the resistance of the photoconductor but not that of the photodiode in the ideal case. An analysis of the discharge characteristics of the photoconductor under high light level conditions and the flood beam bias shows that the discharge rate is exactly the same as without the flood beam except that the photoconductor discharges to the intersection of the current-voltage curve with the flood beam bias, that is to the point where $V = R\, i_{flood}$ where R is the resistance of the photoconductor under the high light level. The rate of current flow through the photoconductor is given by

$$i = \frac{V}{R} = -C\frac{dv}{dt} + i_{flood} \qquad \text{(A-1)}$$

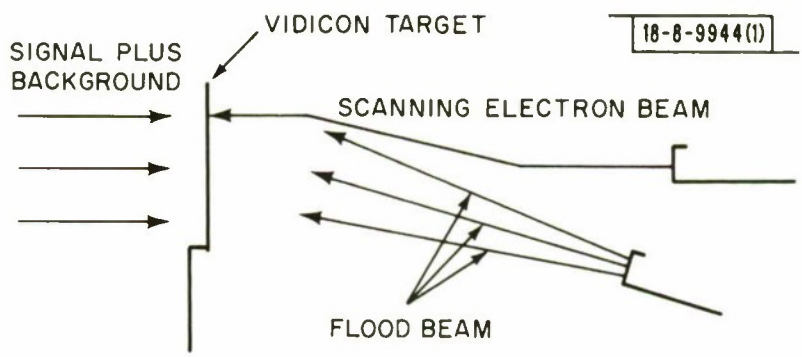

Fig. A-1. Schematic diagram of a vidicon tube equipped with an auxiliary electron flood beam.

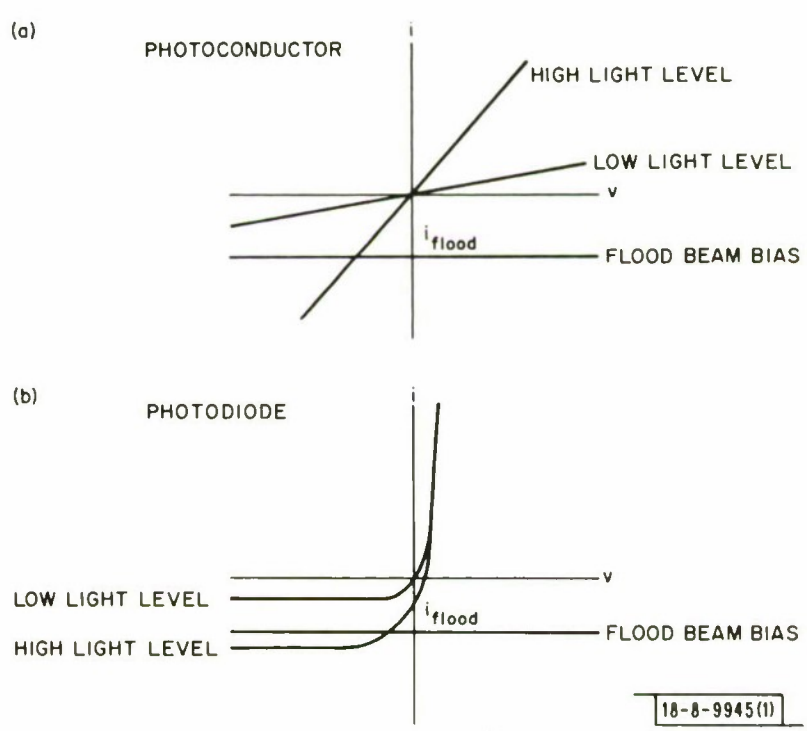

Fig. A-2. Schematic current-voltage characteristics for a vidicon target under low and high levels of illumination showing the effect of a constant current flood beam bias: (a) photoconductive target, (b) photodiode target.

Solving for V(t) we obtain

$$V - R\, i_{flood} = (V_o - R\, i_{flood})e^{-t/RC} \tag{A-2}$$

where V_o is the voltage across the target at time t = 0. The decay rate given by RC is unaffected by the flood beam. The flood beam thus does nothing to increase the integration time and is not helpful in the case of photoconductive vidicon targets. However, in the case of the photodiode the discharge rate is directly controlled by the flood beam. The rate of current flow through the photodiode is given by

$$i = i_s - i_{flood} = -C \frac{dv}{dt} \tag{A-3}$$

where i_s is the reverse saturation current in the presence of the background flux. Equation (A-3) assumes that the diode capacitance is independent of bias voltage which is not true in general, but this does not affect the argument. The voltage decay rate is given by

$$V = V_o - \frac{t}{C}(i_s - i_{flood}) \tag{A-4}$$

The rate of discharge is thus given by the light level induced diode current minus the flood beam bias current. The integration time can therefore be restored by the use of a flood beam in the case of a diode array vidicon target, whereas it cannot be in the case of a photoconductive vidicon target.

B. Photoconductive - Photoemissive Tube

A schematic diagram of a photoconductive - photoemissive tube is shown in Fig. A-3. Ultraviolet light from the light source(6) releases photoelectrons from the photoemitting islands(8). These electrons are extracted by the mesh grid(4), and, depending on their velocity, will or will not pass through the velocity selector grid(7) The velocity of the electrons approaching this grid will be determined by the voltage

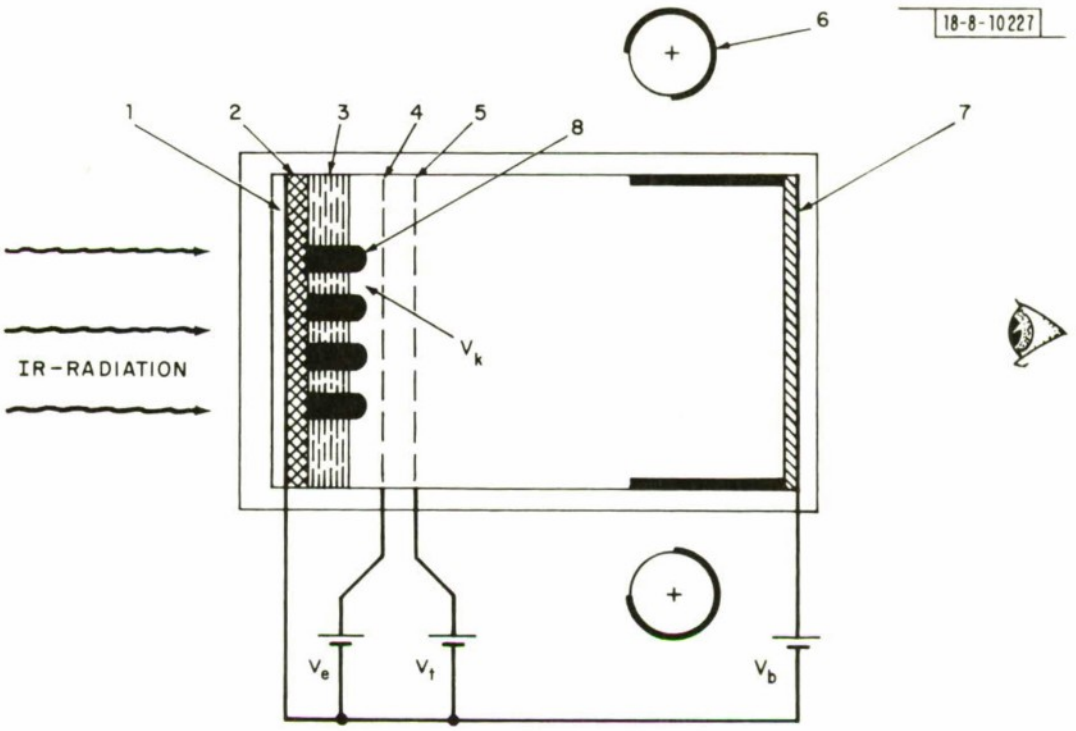

Fig. A-3. Schematic diagram of a photoconductive-photoemissive direct view tube. (1) transparent electrode, (2) photoconductor, (3) multilead plate, (4) extractor mesh grid, (5) velocity selector mesh grid, (6) ultraviolet light source, (7) phosphor screen, (8) photoemitting islands; V_e: potential of extractor mesh grid; V_k: potential of photoemitter; V_t: potential of velocity selector grid; V_b: potential of output phosphor.
(After J. A. Hall, Ref. 10, p. 488.)

drop between the photoemitting islands and the extractor mesh. This voltage is dependent on the intensity of the infrared radiation incident on the photoconductor. The larger the IR signal the larger will be the voltage drop and the higher will be the electron velocity. The bias is then set on the velocity selector grid to just prevent those electrons from passing through whose velocity corresponds to the background infrared photon flux density. An increase in infrared signal results in an increase in electron velocity so that the signal electrons pass through the grid. In the configuration pictured, these electrons impinge on a phosphor screen; however, this could be replaced by an electron current amplifier stage to provide gain.

C. Multiple Scanning Electron Beam Tube

This device utilizes a large number of scanning electron beams, essentially one for each row (line) in the vidicon. Each row of detectors in the delineated target is scanned by a single beam and reads out into a separate amplifier. The total beam current which can be supplied is m times that of the standard vidicon and the bandwidth of each amplifier is m times less than that of the standard vidicon. The array or fan of scanning beams could be provided by a long filament cathode or by an array of small cathodes, for example an array of silicon diode cold cathodes.

APPENDIX B

The integrated background photon flux density for wavelengths between $\lambda = 0$ and $\lambda = \lambda_c$ is given by*

$$Q_b = 2\pi c \int_0^{\lambda_c} \frac{d\lambda}{\lambda^4[\exp(hc/\lambda kT) - 1]} \quad . \tag{B-1}$$

This can be written in the form

$$Q_b = 2\pi c \left(\frac{kT}{hc}\right)^3 \int_{u_c}^{\infty} \frac{u^2 du}{e^u - 1} \tag{B-2}$$

where $u = hc/\lambda kT$. For $u > 1$ this can be expanded

$$Q_b = 2\pi c \left(\frac{kT}{hc}\right)^3 \int_{u_c}^{\infty} \sum_{m=1}^{\infty} e^{-mu} u^2 du \tag{B-3}$$

$$= 2\pi c \left(\frac{kT}{hc}\right)^3 \sum_{m=1}^{\infty} \frac{e^{-mu_c}}{(m)^3} [(mu_c)^2 + 2(mu_c) + 2] \tag{B-4}$$

or replacing $x = 1/u_c = \lambda_c kT/hc$

$$Q_b = 2\pi c\, x/\lambda_c^3 \left\{ \sum_{m=1}^{\infty} \frac{e^{-m/x}}{m} \left(1 + \frac{2x}{m} + 2\frac{x^2}{m^2}\right)\right\} \tag{B-5}$$

For $x_c \ll 1$, Eq. (B-5) can be approximated by retaining just the first term

$$Q_b \simeq 2\pi c x\, (1 + 2x + 2x^2) e^{-1/x} / \lambda_c^3 \quad . \tag{B-6}$$

This is the quantity plotted in Fig. 4. From Eq. (B-6) we can obtain

$$\frac{1}{Q_b} \frac{dQ_b}{dT} = \frac{1}{xT} \frac{(1+3x+6x^2+6x^3)}{(1+2x+2x^2)} \tag{B-7}$$

*Ref. 2, p. 29.

For $x \ll 1$ this gives

$$\frac{1}{Q_b} \frac{dQ_b}{dT} = \frac{1}{xT} (1+x+2x^2) \tag{B-8}$$

For $T = 290^{\circ}K$ the term in parentheses varies from 1.04 for $\lambda_c = 2\ \mu m$ to 1.12 for $\lambda_c = 5\ \mu m$ to 1.46 for λ_c for 14 μm. Equation (B-8) is plotted vs. λ_c for $T = 290^{\circ}K$ in Fig. (B-1).

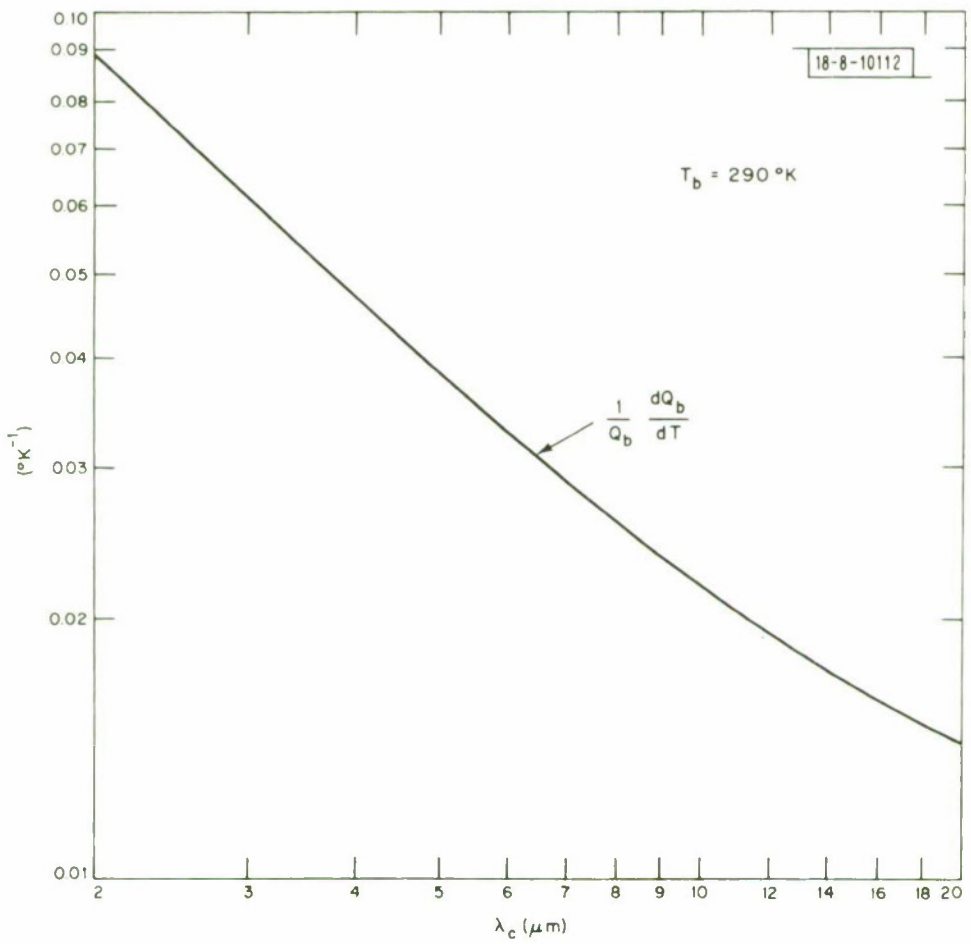

Fig. B-1. Plot of $\frac{1}{Q_b} \frac{dQ_b}{dT}$ vs λ_c for a background temperature of $290^{\circ}K$.

REFERENCES

1. J. A. Hall, Applied Optics 10, 838 (1971).
2. See, for example, P. W. Kruse, L. D. McGlauchlin and R. B. McQuistan, Elements of Infrared Technology (John Wiley & Sons, New York, 1962).
3. J. O. Dimmock, to be published in Proc. of the 13th Annual Conf. of Electronic Materials Committee of Met. Soc. AIME held in San Francisco, 29 August - 1 September 1971.
4. O. H. Schade, Sr., "Theory of Operation and Performance of High Resolution Return-Beam Vidicon Cameras - A Comparison with High-Resolution Photography," Chapter 17, Photoelectronic Imaging Devices, Vol. 2, edited by L. M. Biberman and S. Nudelman (Plenum Press, New York, 1971), p. 421.
5. Ibid, p. 420.
6. Ibid, p. 412 ff.
7. Princeton Applied Research model PAR-225 at 1 MΩ and 200 Hz, Keithley model 103A at 500 KΩ and 3 kHz. Design probably could be optimized for 7.5 kHz and 2MΩ.
8. R. D. Hudson, Jr., Infrared Systems Engineering (Wiley & Sons, New York, 1969).
9. J. A. Jamieson, R. H. McFee, G. N. Plass, R. H. Grube and R. G. Richards, Infrared Physics and Engineering (McGraw-Hill, New York, 1963).
10. J. A. Hall, "Special Sensors," Chapter 20, Photoelectronic Imaging Devices, Vol. 2 edited by L. M. Biberman and S. Nudelman (Plenum Press, New York, 1971), p. 483 ff.

DOCUMENT CONTROL DATA – R&D

(Security classification of title, body of abstract and indexing annotation must be entered when the overall report is classified)

1. ORIGINATING ACTIVITY *(Corporate author)* Lincoln Laboratory, M.I.T.	2a. REPORT SECURITY CLASSIFICATION UNCLASSIFIED 2b. GROUP None
3. REPORT TITLE Capabilities and Limitations of Infrared Vidicons vs Infrared Scanning Systems	
4. DESCRIPTIVE NOTES *(Type of report and inclusive dates)* Technical Note	
5. AUTHOR(S) *(Last name, first name, initial)* Dimmock, John O.	
6. REPORT DATE 3 December 1971	7a. TOTAL NO. OF PAGES 44 7b. NO. OF REFS 10
8a. CONTRACT OR GRANT NO. F19628-70-C-0230 b. PROJECT NO. 649L c. d.	9a. ORIGINATOR'S REPORT NUMBER(S) Technical Note 1971-49 9b. OTHER REPORT NO(S) *(Any other numbers that may be assigned this report)* ESD-TR-71-318
10. AVAILABILITY/LIMITATION NOTICES Approved for public release; distribution unlimited.	
11. SUPPLEMENTARY NOTES None	12. SPONSORING MILITARY ACTIVITY Air Force Systems Command, USAF

13. ABSTRACT

The performances of infrared television camera tubes and infrared scanning systems are compared as a function of background photon flux density. The two-dimensional vidicon is found to be superior in performance at low background photon flux levels, below about 10^{12} photons/sec cm^2. At higher background levels, for application to terrestrial scenes in the 3 to 5 μm region (flux densities of $\sim 10^{13}$ to 10^{16} photons/sec cm^2) the two-dimensional vidicon is generally less sensitive than the linear array if variations in the vidicon target responsivity exceed about 0.05%. In addition, background suppression or compensation must be achieved through the use of either an electron flood beam or a photoconductive-photoemissive tube. Even if this is done, the contrast available in the vidicon appears marginal for terrestrial scenes. The situation in the 8 to 14 μm range (flux densities of 10^{18} photons/sec cm^2) is two orders of magnitude more difficult.

14. KEY WORDS

vidicons
scanning systems
photon
flux density
infrared